

# Construction of $bb\bar{u}\bar{d}$ tetraquark states on lattice with NRQCD bottom and HISQ up/down quarks

Protick Mohanta and Subhasish Basak

*School of Physical Sciences, National Institute of Science  
Education and Research, HBNI, Odisha 752050, India*

(Dated: November 24, 2020)

## Abstract

We construct  $bb\bar{u}\bar{d}$  states on lattice using NRQCD action for bottom and HISQ action for the light up/down quarks. The NRQCD-HISQ tetraquark operators are constructed for “bound”  $[bb][\bar{u}\bar{d}]$  and “molecular”  $[b\bar{u}][b\bar{d}]$  states. Corresponding to these different operators, two different appropriately tuned light quark masses are needed to obtain the desired spectra. We explain this requirement of different  $m_{u/d}$  in the light of relativised quark model involving Hartree-Fock calculation. The mass spectra of double bottom tetraquark states are obtained on MILC  $N_f = 2 + 1$  Asqtad lattices at three different lattice spacings. Variational analysis has been carried out to obtain the relative contribution of “bound” and “molecular” states to the energy eigenstates.

## I. INTRODUCTION

The multi-quark hadronic states other than the mesons and baryons are relatively new entrants particularly in the heavy quark sector. The signature of some of such states containing four or more quarks and/or antiquarks have been observed in experiments [1–6]. The QCD states composed of four valence quarks are popularly referred to as tetraquark, which is used to denote either bound or often both bound and two 2-quark mesonic particles bound in a molecular like structure. In this paper we use the term tetraquark in the latter sense. Such states are characterized by  $J^{PC}$  quantum numbers that cannot be arrived at from the quark model. However, heavy hadronic tetraquark states  $QQ\bar{l}\bar{l}$  and their stability in the infinite quark mass limit had been studied in [7, 8] which raised the possibility of existence of heavy four quark bound states below the  $Q\bar{l} - Q\bar{l}$  threshold. Of late, the observations of  $Z^-(4430, 1^+)$  of minimal quark content being  $c\bar{c}d\bar{u}$  [3] have been reported along with the  $1^+$  states like  $Z_b(10610)$  and  $Z'_b(10650)$ , having minimal quark content of four quarks (containing a  $b\bar{b}$  pair) that are a few MeV above the thresholds of  $B^*\bar{B}$  (10604.6) and  $B^*\bar{B}^*$  (10650.2) [1, 2]. The proximity of  $Z_b, Z'_b$  to the  $B^*\bar{B}^*$  threshold values perhaps suggest molecular, instead of bound, nature of the states.

Around the same time, lattice QCD has been employed to investigate the bound and/or molecular nature of the heavy tetraquark states, not only to understand the above experimentally observed states but also to identify other possible bound tetraquark states in both  $0^+$  and  $1^+$  channels. In the context of lattice study of heavy tetraquarks, some early lattice calculations in charm sector involve  $T_{cc}$  and  $T_{cs}$  tetraquark states [9],  $cc\bar{c}\bar{c}$  [10],  $X(3872)$  and  $Y(4140)$  [11] and more recently  $D_{s0}^*(2317)$  [12]. The bottom sector too received intense attention in the past few years. However, on the lattice the  $Z_b, Z'_b$  of quark content  $[b\bar{b}u\bar{d}]$  has been replaced with relatively simpler  $[b\bar{b}u\bar{d}]$  or equivalently  $[\bar{b}b\bar{u}d]$  system; that is to say instead of  $B^*\bar{B}$  or  $B^*\bar{B}^*$ , the study is basically on  $BB^* / B^*B^*$  systems. One exploratory lattice study of the  $[b\bar{b}u\bar{d}]$  system has been reported in [13]. The lattice investigations this far involve four bottom  $b\bar{b}b\bar{b}$  [14] and two bottom tetraquark states  $\bar{b}b\bar{l}_1l_2$ , where  $l_1, l_2 \in c, s, u, d$ , [15–18]. An important observation of these lattice studies is that the possibility of the existence of  $b\bar{b}\bar{l}_1\bar{l}_2$  tetraquark bound states increases with decreasing light quark masses, while they become less bound with decreasing heavy (anti)quark mass.

Besides the usual lattice simulations, the heavy tetraquark systems have also been studied

using QCD potential [19] and Born-Oppenheimer approximation [20–23]. The main idea in these references is to investigate tetraquark states with two heavy (anti)quarks, which was  $\bar{b}\bar{b}$  in the study, and two lighter quarks using quantum mechanical Hamiltonian containing screened Coulomb potential. This approach has been used to explain our two different choices of light  $u/d$  quark masses for different classes of tetraquark operators.

In this work our goal is to construct tetraquark states, having quark content  $bb\bar{l}_1\bar{l}_2$  in  $1^+$  both below and above  $B - B^*$  threshold, by a combination of lattice operators and tuning quark masses based on quantum mechanical potential calculation. For the  $b$  quark, we employed nonrelativistic QCD formulation [24, 25], as is the usual practice, and HISQ action [26] for  $l_1, l_2 = u/d$ . Here we also explore through variational/GEVP analysis how the trial states created by our operators contribute to the energy eigenstates.

First, we briefly review the salient features and parameters of both NRQCD and HISQ actions along with the steps involve in combining the relativistic  $u/d$  HISQ propagators with the NRQCD  $b$  quark propagators in the section II. We have considered two different kind of operators – the local heavy diquark and light antidiquark (often referred as “good diquark” configuration) and molecular meson-meson, we described these constructions in the section III. We collect our spectrum results in section IV that contains subsections on quark mass tuning (IV A), Hartree-Fock calculation of two light quarks in the presence of a heavy quark (IV B), tetraquark spectra (IV C) and GEVP analysis (IV D). Finally we summarized our results in section V.

## II. QUARK ACTIONS

Lattice QCD simulations with quarks require quark mass to be  $am_l \ll 1$ , where  $a$  is the lattice spacing. In the units of the lattice spacings presently available, the  $b$  quark mass is not small *i.e.*  $am_b \not\ll 1$ . As is generally believed, the typical velocity of a  $b$  quark inside a hadron is nonrelativistic  $v^2 \sim 0.1$  and is much smaller than the bottom mass. This makes NRQCD our action of choice for  $b$  quarks on lattice. We have used  $\mathcal{O}(v^6)$  NRQCD action [25], where the Hamiltonian is  $H = H_0 + \delta H$ , where  $H_0$  is the leading  $\mathcal{O}(v^2)$  term, the  $\mathcal{O}(v^4)$

and  $\mathcal{O}(v^6)$  terms are in  $\delta H$  with coefficients  $c_1$  through  $c_7$ ,

$$H_0 = -\frac{\tilde{\Delta}^2}{2m_b} - \frac{a}{4n} \frac{(\Delta^2)^2}{4m_b^2} \quad (1)$$

$$\begin{aligned} \delta H = & -c_1 \frac{(\Delta^2)^2}{8m_b^3} + c_2 \frac{ig}{8m_b^2} \left( \vec{\Delta}^\pm \cdot \vec{E} - \vec{E} \cdot \vec{\Delta}^\pm \right) - c_3 \frac{g}{8m_b^2} \vec{\sigma} \cdot \left( \vec{\Delta}^\pm \times \vec{E} - \vec{E} \times \vec{\Delta}^\pm \right) \\ & - c_4 \frac{g}{2m_b} \vec{\sigma} \cdot \vec{B} - c_5 \frac{g}{8m_b^3} \left\{ \Delta^2, \vec{\sigma} \cdot \vec{B} \right\} - c_6 \frac{3g}{64m_b^4} \left\{ \Delta^2, \vec{\sigma} \cdot \left( \vec{\Delta}^\pm \times \vec{E} - \vec{E} \times \vec{\Delta}^\pm \right) \right\} \\ & - c_7 \frac{ig^2}{8m_b^3} \vec{\sigma} \cdot \vec{E} \times \vec{E} \end{aligned} \quad (2)$$

where  $\Delta^\pm$  and  $\Delta^2$  are discretized symmetric covariant derivative and lattice Laplacian respectively. Both the derivatives are  $\mathcal{O}(a^4)$  improved as are the chromoelectric  $\vec{E}$  and chromomagnetic  $\vec{B}$  fields. The  $b$  quark propagator is generated by time evolution of the Hamiltonian  $H$ ,

$$G(\vec{x}, t+1; 0, 0) = \left( 1 - \frac{aH_0}{2n} \right)^n \left( 1 - \frac{a\delta H}{2} \right) U_4(\vec{x}, t)^\dagger \left( 1 - \frac{a\delta H}{2} \right) \left( 1 - \frac{aH_0}{2n} \right)^n G(\vec{x}, t; 0, 0) \quad (3)$$

$$\text{with } G(\vec{x}, t; 0, 0) = \begin{cases} 0 & \text{for } t < 0 \\ \delta_{\vec{x}, 0} & \text{for } t = 0 \end{cases}$$

The tree level value of all the coefficients  $c_1, c_2, c_3, c_4, c_5, c_6$  and  $c_7$  is 1. Here  $n$  is the factor introduced to ensure numerical stability at small  $am_b$ , where  $n > 3/2m_b$  [24].

In NRQCD, the rest mass term does not appear either in the equation (1) or in (2), and therefore, hadron masses cannot be determined from their energies at zero momentum directly from the exponential fall-off of their correlation functions. Instead, we calculate the kinetic mass  $M_k$  of heavy-heavy mesons from its energy-momentum relation, which to  $\mathcal{O}(p^2)$  is [27],

$$E(p) = E(0) + \sqrt{p^2 + M_k^2} - M_k \quad \Rightarrow \quad E(p)^2 = E(0)^2 + \frac{E(0)}{M_k} p^2. \quad (4)$$

where  $M_k$  is the kinetic mass of the meson which is calculated considering  $E(p)$  at different values of lattice momenta  $\vec{p} = 2\vec{n}\pi/L$ . The  $b$  quark mass is tuned from the spin average of kinetic masses of  $\Upsilon$  and  $\eta_b$ , and matching them with the experimental spin average value,

$$M_{b\bar{b}} = \frac{3M_\Upsilon + M_{\eta_b}}{4} \quad (5)$$

The experimental value to which  $M_{b\bar{b}}$  is tuned to, however, is not 9443 MeV that is obtained from spin averaging  $\Upsilon$  (9460 MeV) and  $\eta_b$  (9391 MeV) experimental masses, but to an

appropriately adjusted value of 9450 MeV [28], which we denote as  $M_{\text{phys}}^{\text{mod}}$  in the equation (6) below. The hadron mass is then obtained from

$$M_{\text{latt}} = E_{\text{latt}} + \frac{n_b}{2} (M_{\text{phys}}^{\text{mod}} - E_{\text{latt}}^{\eta_b}) \quad (6)$$

where  $E_{\text{latt}}$  is the lattice zero momentum energy in MeV,  $n_b$  is the number of  $b$ -quarks in the bottom hadron.

The  $u/d$  light quarks comfortably satisfy the criteria  $am_l \ll 1$  and, therefore, we can use a relativistic lattice action. We use HISQ action for the  $u/d$  quarks, which is given in [26],

$$\mathcal{S} = \sum_x \bar{q}(x) (\gamma^\mu D_\mu^{\text{HISQ}} + m) q(x) \quad \text{where,} \quad D_\mu^{\text{HISQ}} = \Delta_\mu(W) - \frac{a^2}{6}(1 + \epsilon) \Delta_\mu^3(x). \quad (7)$$

Because HISQ action reduces  $\mathcal{O}(\alpha_s a^2)$  discretization error found in Asqtad action, it is well suited for  $u/d$  (and  $s$ ) quarks. The parameter  $\epsilon$  in the coefficient of Naik term can be appropriately tuned to use the action for  $c$  quarks, which we do not have here. For  $u/d$  (and  $s$ ) quarks, the  $\epsilon = 0$ .

HISQ action is diagonal in spin space, and therefore, the corresponding quark propagators do not have any spin structure. The full  $4 \times 4$  spin structure is regained by multiplying the propagators by Kawamoto-Smit multiplicative phase factor [29],

$$\Omega(x) = \prod_{\mu=1}^4 (\gamma_\mu)^{x_\mu} = \gamma_1^{x_1} \gamma_2^{x_2} \gamma_3^{x_3} \gamma_4^{x_4}. \quad (8)$$

### III. TETRAQUARK OPERATORS

In the present paper, we have considered two kinds of tetraquark operators – the local heavy diquark and light antidiquark and molecular meson-meson. The  $b$  quark, being nonrelativistic, is expressed in terms of two component field  $\psi_h$ . We convert it into a four component spinor  $Q$  having vanishing two lower components,

$$Q \equiv \begin{pmatrix} \psi_h \\ 0 \end{pmatrix} \quad (9)$$

which help us to combine  $b$  field and relativistic four component light quark fields in the usual way. The heavy-light meson operator, that we will make use of in the operator construction, is written as

$$\mathcal{O}_{hl}(x) = \bar{Q}(x) \Gamma l(x) \quad (10)$$

where  $l(x)$  stands for the light quark fields,  $\bar{Q} = Q^\dagger \gamma_4$  and depending on pseudoscalar and vector mesons  $\Gamma = \gamma_5$  and  $\gamma_i$  respectively.

Because of the vanishing lower components, the states with  $Q$  can only be projected to the positive parity states. The local double bottom tetraquark operators that we can construct for  $bb\bar{l}_1\bar{l}_2$  system are,

$$\mathcal{O}_{M_1} \equiv \mathcal{O}_{B^*B} = [\bar{l}_1(x)\gamma_i Q(x)] [\bar{l}_2(x)\gamma_5 Q(x)], \quad (11)$$

$$\mathcal{O}_{M_2} \equiv \mathcal{O}_{B^*B^*} = \epsilon_{ijk} [\bar{l}_1(x)\gamma_j Q(x)] [\bar{l}_2(x)\gamma_k Q(x)], \quad (12)$$

$$\mathcal{O}_D \equiv \mathcal{O}_{\mathcal{Q}^*\tilde{\pi}} = [Q^{aT}(x)C\gamma_i Q^b(x)] [\bar{l}_1^a(x)C\gamma_5\bar{l}_2^bT(x)] \quad (13)$$

where  $l_1 \neq l_2$  and  $l_1, l_2 \in u, d$ . The  $a, b$  are the color indices. The naming convention above is borrowed from reference [16] but the exact construction of the operators is different. In literature the operators in (11) and (12) are often referred to as ‘‘molecular’’. In this work we have not included the non-local operators in our GEVP analysis like those in [18], although they will admittedly effect the first few excited states.

The diquark-antidiquark  $1^+$  four quark state  $bb\bar{l}_1\bar{l}_2$  with  $l_1 \neq l_2$  in (13) can actually be defined in two ways [30],

$$\begin{aligned} \mathcal{O}_{\mathcal{Q}^*\tilde{\pi}} &= [Q^{aT}C\gamma_i Q^b] [\bar{l}_1^a C\gamma_5\bar{l}_2^bT - \bar{l}_1^b C\gamma_5\bar{l}_2^aT] \\ \mathcal{O}_{\mathcal{Q}\tilde{\pi}^*} &= [Q^{aT}C\gamma_5 Q^b] [\bar{l}_1^a C\gamma_i\bar{l}_2^bT + \bar{l}_1^b C\gamma_i\bar{l}_2^aT] \end{aligned} \quad (14)$$

The subscripts  $\mathcal{Q}^*$  and  $\tilde{\pi}$  in the operator  $\mathcal{O}_{\mathcal{Q}^*\tilde{\pi}}$  are in  $\bar{3}_c$  and  $3_c$  respectively, while  $\mathcal{Q}$  and  $\tilde{\pi}^*$  in the operator  $\mathcal{O}_{\mathcal{Q}\tilde{\pi}^*}$  are in  $6_c$  and  $\bar{6}_c$ . But both  $\mathcal{O}_{\mathcal{Q}^*\tilde{\pi}}$  and  $\mathcal{O}_{\mathcal{Q}\tilde{\pi}^*}$  correspond to the  $1^+$  state. Of these the  $\mathcal{O}_{\mathcal{Q}^*\tilde{\pi}}$  is our desired ‘‘bound’’ tetraquark operator because one-gluon-exchange interaction is attractive for a heavy quark pair in  $\bar{3}_c$  diquark configuration [8] and spin dependent attraction exists for light quark pairs in ‘‘good diquark’’ configuration characterized by color  $\bar{3}_c$ , spin  $J = 0$  and isospin  $I = 0$  or  $1/2$  [31]. The two terms in  $\mathcal{O}_{\mathcal{Q}^*\tilde{\pi}}$  contribute identically in the final correlator, hence we consider only the first term in the calculation. The generic form of the temporal correlation among the operators at zero momentum is,

$$C_{XY}(t) = \sum_{\mathbf{x}} \langle [\mathcal{O}_X(\mathbf{x}, t)] [\mathcal{O}_Y(\mathbf{0}, 0)]^\dagger \rangle, \quad (15)$$

where  $X, Y$  can be any of  $D, M_1, M_2$  in equations (11), (12) and (13). For example, the explicit forms of the zero momentum correlators, including cross-correlator, when  $X$  and  $Y$

are  $M_1 = B^* B$  and  $D = \mathcal{Q}^* \tilde{\pi}$ , are

$$C_{M_1 M_1}(t) = \sum_{\vec{x}} \text{Tr} \left[ \gamma_5 M_1^\dagger(x, 0) \gamma_5 \gamma_i G(x, 0) \gamma_i \right] \times \text{Tr} \left[ M_2^\dagger(x, 0) G(x, 0) \right] \\ - \sum_{\vec{x}} \text{Tr} \left[ G(x, 0) M_2^\dagger(x, 0) G(x, 0) \gamma_i \gamma_5 M_1^\dagger(x, 0) \gamma_5 \gamma_i \right] \quad (16)$$

$$C_{DD}(t) = \sum_{\vec{x}} \text{Tr} \left[ (G^{ad}(x, 0))^T \gamma_i \gamma_4 \gamma_2 G^{bc}(x, 0) \gamma_4 \gamma_2 \gamma_i \right] \times \\ \text{Tr} \left[ \gamma_4 \gamma_2 M_1^{\dagger da}(x, 0) \gamma_4 \gamma_2 \left( \gamma_5 M_2^{\dagger cb}(x, 0) \gamma_5 \right)^T \right] \quad (17)$$

$$C_{DM_1}(t) = \sum_{\vec{x}} \text{Tr} \left[ G^{ad}(x, 0) \gamma_i \gamma_5 M_1^{\dagger da}(x, 0) \gamma_5 \gamma_2 \gamma_4 \gamma_5 \right]_{\mu\nu} \times \\ \text{Tr} \left[ \gamma_2 \gamma_i \gamma_4 G^{bc}(x, 0) \gamma_5 \gamma_5 M_2^{\dagger cb}(x, 0) \gamma_5 \right]_{\mu\nu} \quad (18)$$

Above in the equations (17) and (18), traces and transposes are taken over the spinor indices, while in the equation (16) the traces are taken over both the spinor and color indices. Here  $G(x, 0)$  denotes the heavy quark propagators while the  $M(x, 0)$  are the light quark propagators. The term  $\text{Tr} \left[ G M_2^\dagger G M_1^\dagger \right]$  appears only in  $C_{M_1 M_1}$ ,  $C_{M_2 M_2}$ ,  $C_{M_1 M_2}$  and  $C_{M_2 M_1}$  correlators. The diquark and the anti-diquark part of  $\mathcal{O}_D$  in (13) do not have free spinor index and, therefore, we do not have similar  $\text{Tr} \left[ G M_2^\dagger G M_1^\dagger \right]$  term in  $C_{DD}$ . The remaining correlators  $C_{DM_1}$ ,  $C_{DM_2}$ ,  $C_{M_1 D}$  and  $C_{M_2 D}$  can not be expressed in compact  $\text{Tr} \left[ G M_1^\dagger \right] \times \text{Tr} \left[ G, M_2^\dagger \right]$  form. In terms of coding, we have to keep in mind that NRQCD and MILC library suit use different representation of gamma matrices. Therefore the heavy quark propagator  $G(x, 0)$  has to be rotated to the MILC basis before implementing the equations (16), (17) and (18). The unitary matrix needed to do this transformation is given by [32],

$$S \gamma_\mu^{\text{MILC}} S^\dagger = \gamma_\mu^{\text{NR}} \quad \text{where,} \quad S = \frac{1}{\sqrt{2}} \begin{pmatrix} \sigma_y & \sigma_y \\ -\sigma_y & \sigma_y \end{pmatrix}. \quad (19)$$

#### IV. NUMERICAL STUDIES

We calculated the double bottom tetraquark spectra using the publicly available  $N_f = 2 + 1$  Asqtad gauge configurations generated by MILC collaboration. Details about these lattices can be found in [33]. It uses Symanzik-improved Lüscher-Weisz action for the gluons and Asqtad action [34, 35] for the sea quarks. The lattices we choose have a fixed ratio of  $am_l/am_s = 1/5$  with lattice spacings 0.15 fm, 0.12 fm and 0.09 fm and they correspond to

the same physical volume. We have not determined the lattice spacings independently but use those given in [33]. In the Table I we listed the ensembles used in this work.

TABLE I: MILC  $N_f = 2 + 1$  Asqtad configurations used in this work. The gauge coupling is  $\beta$  and the lattice spacing is  $a$ . The  $u/d$  and  $s$  sea quark masses are  $m_l$  and  $m_s$  respectively and the lattice size is  $L^3 \times T$ . The  $N_{\text{cfg}}$  is number of configurations used in this work.

$\beta = 10/g^2$	$a(\text{fm})$	$am_l$	$am_s$	$L^3 \times T$	$N_{\text{cfg}}$
6.572	0.15	0.0097	0.0484	$16^3 \times 48$	600
6.76	0.12	0.0100	0.0500	$20^3 \times 64$	600
7.09	0.09	0.0062	0.0310	$28^3 \times 96$	300

### A. Quark mass tuning

For  $bb\bar{u}\bar{d}$  mass calculation, we need nonperturbative tuning of both  $m_b$  and  $m_{u/d}$ . With the help of equation (5), the tuning of  $m_b$  has been carried out by calculating the spin average of  $\Upsilon$  and  $\eta_b$  kinetic masses and comparing the same with the spin average and suitably adjusted experimental  $\Upsilon$  and  $\eta_b$  masses as discussed in section II. The tuned bare  $am_b$  quark masses for lattices used in this work are given in Table II.

TABLE II: Tuned  $b$  and  $u/d$  quark bare masses for lattices used in this work. For  $u/d$ -quark mass, we mention the particle states used to tune.

Quark	Tuning	$16^3 \times 48$	$20^3 \times 64$	$28^3 \times 96$
	hadron	(0.15 fm)	(0.12 fm)	(0.09 fm)
$am_b$	$\Upsilon - \eta_b$	2.76	2.08	1.20
$am_{u/d}$	$\Lambda_b$ (5620)	0.105	0.083	0.064
$am_{u/d}$	$B$ (5280)	0.155	0.118	0.087

But the tuning of  $am_{u/d}$  is rather tricky. It was found in [32] that the  $B$ -meson tuned  $am_{u/d}$  reproduces the mass of  $\Sigma_b$  baryon but not that of  $\Lambda_b$ . Therefore, we tuned  $am_{u/d}$  to

two different values depending on the construction of the pairs  $[ud]$  and  $[bu]$  or  $[bd]$ . The motivation to do so followed from the observation that substantial mass difference exist among singly heavy baryons having same quark content and same  $J^P$ . For instance, the mass differences between the  $J^P = \frac{1}{2}^+$  pairs  $(\Lambda_b, \Sigma_b [bdu])$ ,  $(\Lambda_c, \Sigma_c [cd u])$ ,  $(\Xi_b, \Xi'_b [bsu])$  and  $(\Xi_c, \Xi'_c [csu])$  are in the range 110–190 MeV. The  $\Lambda_b, \Lambda_c, \Xi_b$  and  $\Xi_c$  baryons are characterized by the spin of the  $[l_1 l_2]$  (where  $l_{1,2} \in u, d, s$ ) light-light diquark  $s_l = 0$  while  $\Sigma_b, \Sigma_c, \Xi'_b$  and  $\Xi'_c$  by  $s_l = 1$ . This differences in their wave functions alone cannot generate such mass differences [36] but can at most account for a difference of about 30 MeV. The heavy hadron chiral perturbation theory calculations [37, 38] for  $\Lambda_Q$  and  $\Sigma_Q$ , where  $Q \in b, c$ , demonstrated that the mass differences get large correction of the order  $\approx 150$  MeV. A correction of similar magnitude is anticipated in our NRQCD-HISQ heavy baryon / tetraquark systems, but the relevant  $\chi$ PT for which is yet to be available. To include such a correction in our calculations, we propose this unique method of tuning the  $[\bar{u}\bar{d}]$  diquark system to  $\Lambda_b$ -baryon and  $[b\bar{u}]$  to  $B$ -meson.

In the present paper, we try to understand this tuning scheme in more details with the help of relativised quark model [39, 40] and Hartree-Fock calculation. The basic idea is that  $am_{u/d}$  has to be tuned to two different values corresponding to two different constructions of the pairs  $[\bar{u}\bar{d}]$  and  $[b\bar{u}]$ . In the operator  $\mathcal{O}_D \equiv [bb][\bar{u}\bar{d}]$ , the anti-diquark part formed with two light  $u/d$  quarks is the same that appear in the baryonic operator  $\Lambda_b \equiv (u^T C \gamma_5 d) b$ , and hence, we use experimental  $\Lambda_b$  mass 5620 MeV to tune the bare  $am_{u/d}$ . For the operators  $\mathcal{O}_{M_1/M_2}$ , the diquark part is formed between heavy quark and light antiquark  $[b\bar{u}]$  which is the same as in the  $B$ -meson  $(\bar{b}\gamma_{(5,k)} u)$  or  $\Sigma_b \equiv (Q^T C \gamma_5 u) u$ . In such case we tend to use  $B$ -meson mass 5279 MeV to tune the  $am_{u/d}$ .

For  $\mathcal{O}_D$  we have exclusively used  $am_{u/d}$  tuned from  $\Lambda_b$  where as for determining the lattice tetraquark thresholds  $B - B^*$  it is  $B$  tuned. But  $\mathcal{O}_D, \mathcal{O}_{M_1}, \mathcal{O}_{M_2}$  all have the same quantum numbers and, therefore, expected to mix and contribute to the finite volume lattice “bound” states. When looking for such bound states, we will be using  $\Lambda_b$  tuned  $am_{u/d}$  for all the operators. However, while searching for purely molecular states, in light of Hartree-Fock calculation in section IV B below we entirely omit  $\mathcal{O}_D$  and worked only with the  $\mathcal{O}_{M_1/M_2}$  operators using just the  $B$  tuning.

This differently tuned  $am_{u/d}$  gave consistent result in [32] and expect to repeat the same in this work. The results of  $u/d$  quark mass tuning that are made use of in this work is

given in the Table II.

Before we calculate the spectra of the  $|D\rangle$ ,  $|M_1\rangle$ ,  $|M_2\rangle$  tetraquark states defined in subsection IV C, in the following subsection IV B we try to understand the diquark dependent different tuning of the light  $u/d$  quark masses. For this we consider Schrödinger Hamiltonian for (a) hydrogen-like system, namely  $B$  meson with an  $\bar{u}$  antiquark in the potential of a static  $b$  quark and (b) helium-like system, which is  $\Lambda_b$  baryon with  $u$ ,  $d$  quarks in the same  $b$  quark field.

### B. Hartree-Fock calculation of tetraquark states

In order to gain a qualitative understanding of two different tunings of  $m_{u/d}$ , we consider the light antiquark and light-light diquark in the potential of heavy, nearly static color source, the  $b$  quark(s). This picture is akin to hydrogen and helium-like quantum mechanical systems. For the molecular tetraquark states, the basic assumption is that the light antiquark wave functions do not have significant overlap with each other and they are effectively in the potential of their respective heavy  $b$  quarks [21] i.e. a two  $B$ -meson like system. But for the diquark-antidiquark tetraquark state  $[bb][\bar{u}\bar{d}]$  where antidiquark component is similar to the  $\Lambda_b$  light-light diquark, we tune the  $u/d$  quark mass using the  $\Lambda_b$  baryon. The situation is depicted schematically in Figs. 1 and 2. The relevant interpolating operators for  $\Lambda_b$  and  $B$  meson are fairly standard but for HISQ light quarks a whole array of bottom baryon operators, including  $\Lambda_b$  can be found in [32].

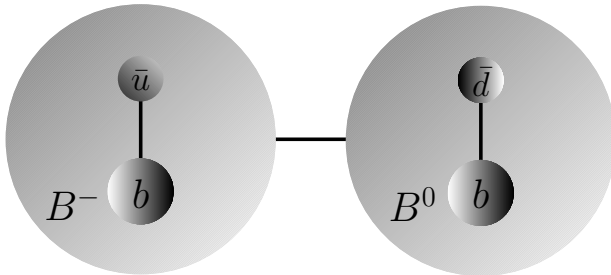


FIG. 1: Molecular tetraquark state viewed as bound state of two  $B$  mesons, which is similar to two hydrogen atoms forming a hydrogen molecule.

The relativised quark model [39, 40] helps us to numerically calculate the masses of  $B$  meson and  $\Lambda_b$  baryon using the light (anti)quark mass as parameter. The molecular tetraquark state can be visualized as two  $B$  meson molecule as shown in the Fig. 1. Then for each  $B$  meson, the light  $u/d$  antiquark is taken to be in the field of “static”  $b$  quark and we solve the problem by considering the radial part of the Schrödinger equation numerically using suitably modified Herman-Skillman code [41].

$$-\frac{1}{2m_{u/d}} \frac{d^2 U(r)}{dr^2} + V(r)U(r) = EU(r) \quad (20)$$

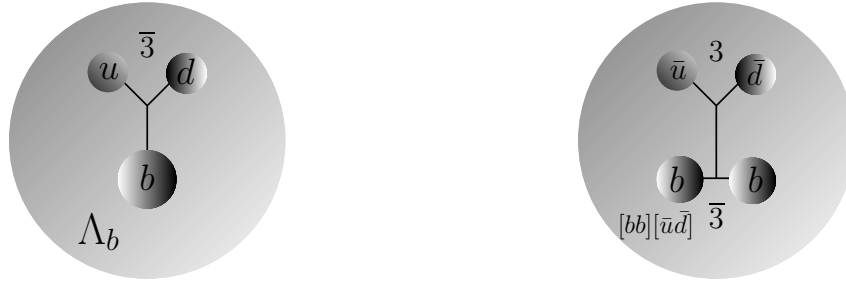
Here  $U(r) = r\psi(r)$  and the potential  $V(r)$  is given by

$$V(r) = -\frac{4\alpha}{3r} + \beta r \quad (21)$$

The  $B$  meson mass  $M_B$  is, therefore, determined from the energy eigenvalue  $E$ ,

$$M_B = m_b + m_{u/d} + E \quad (22)$$

where  $m_b = 4.18$  GeV ( $\overline{\text{MS}}$ ) is the mass of the bottom quark, the  $\alpha = \pi/16$  [22] and  $\beta = 0.18$  GeV<sup>2</sup> [39]. For  $M_B = 5.279$  GeV, the light quark mass obtained is  $m_{u/d} \approx 0.227$  GeV.



(a)  $u/d$  quarks in  $\Lambda_b$  baryons form a  $\bar{3}_c$  diquark in presence of a  $b$  quark. (b) Like  $\Lambda_b$ , two  $b$  quarks form a (nearly) static nucleus surrounded by  $\bar{u}, \bar{d}$  cloud.

FIG. 2: Schematic diagram of helium-like  $\Lambda_b$  and  $[bb][\bar{u}\bar{d}]$  tetraquark state used for Hartree-Fock treatment.

For  $\Lambda_b$  baryon, we used Hartree-Fock method [42, 43] to solve the helium-like Hamiltonian,

$$H = -\frac{1}{2m_{u/d}} \nabla_1^2 - \frac{2\alpha}{3r_1} + \frac{\beta r_1}{2} - \frac{1}{2m_{u/d}} \nabla_2^2 - \frac{2\alpha}{3r_2} + \frac{\beta r_2}{2} - \frac{2\alpha'}{3r_{12}} + \frac{\beta' r_{12}}{2} \quad (23)$$

where  $r_{12}$  is the relative distance between two light quarks “orbiting” the heavy quark and their interaction potential is the last two terms in the equation (23) with coefficient  $\alpha'$  and  $\beta'$ . For the Hartree-Fock calculation of the energy  $E$ , we take  $\beta' = \beta$  and  $\alpha' = 0.6$  [39].

To solve the Hamiltonian (23), we consider the trial wave function, which is space-symmetric and spin-antisymmetric, in terms of Slater determinant

$$\Psi^{\text{HF}} = \frac{1}{\sqrt{2}} \begin{vmatrix} \chi_1(x_1) & \chi_1(x_2) \\ \chi_2(x_1) & \chi_2(x_2) \end{vmatrix}, \quad (24)$$

where  $x_i \equiv (\vec{r}, s)$  collectively denotes the space and spin indices,  $\chi_i(\vec{r}, s) = \phi_{i,s}(\vec{r}) \mathcal{S}(s)$  with  $\phi(\vec{r})$  being the 1S state. Therefore, the expectation value of the the Hamiltonian can be written as

$$\begin{aligned} \langle \Psi^{\text{HF}} | H | \Psi^{\text{HF}} \rangle &= \langle T \rangle + \int \rho(\vec{r}) V_{\text{ext}}(\vec{r}) d\vec{r} - \frac{Z'}{2} \iint \frac{\rho(\vec{r})\rho(\vec{r}_1)}{|\vec{r} - \vec{r}_1|} d\vec{r} d\vec{r}_1 \\ &+ \frac{B'}{2} \iint \rho(\vec{r}) \rho(\vec{r}_1) |\vec{r} - \vec{r}_1| d\vec{r} d\vec{r}_1 \\ &+ \frac{Z'}{2} \sum_{i,j,s} \iint \frac{\phi_{i,s}^*(\vec{r}) \phi_{j,s}^*(\vec{r}_1) \phi_{i,s}(\vec{r}_1) \phi_{j,s}(\vec{r})}{|\vec{r} - \vec{r}_1|} d\vec{r} d\vec{r}_1 \\ &- \frac{B'}{2} \sum_{i,j,s} \iint \phi_{i,s}^*(\vec{r}) \phi_{j,s}^*(\vec{r}_1) \phi_{i,s}(\vec{r}_1) \phi_{j,s}(\vec{r}) |\vec{r} - \vec{r}_1| d\vec{r} d\vec{r}_1 \end{aligned} \quad (25)$$

where, we have used

$$\begin{aligned} \langle T \rangle &= \sum_{i,s} \left\langle \phi_{i,s}(\vec{r}) \left| -\frac{1}{2m_{u/d}} \nabla^2 \right| \phi_{i,s}(\vec{r}) \right\rangle \\ \rho(\vec{r}) &= \sum_{i,s} |\phi_{i,s}(\vec{r})|^2, \quad V_{\text{ext}}(\vec{r}) = -\frac{2\alpha}{3r} + \frac{\beta r}{2} \\ Z' &= \frac{2\alpha'}{3} \quad \text{and} \quad B' = \frac{\beta'}{2}. \end{aligned}$$

In contrast to the helium atom, the presence of linear  $r$ -terms in the Hamiltonian leads to additional exchange-energy terms in the calculation. With these linear  $r$ -terms in, the Hartree-Fock equation becomes

$$\begin{aligned} E \phi_{i,s}(\vec{r}) &= \left[ -\frac{1}{2m_{u/d}} \nabla^2 + V_{\text{ext}}(\vec{r}) - Z' \int \frac{\rho(\vec{r}_1)}{|\vec{r} - \vec{r}_1|} d\vec{r}_1 + B' \int \rho(\vec{r}_1) |\vec{r} - \vec{r}_1| d\vec{r}_1 \right] \phi_{i,s}(\vec{r}) \\ &- B' \sum_{j,s} \int \phi_{j,s}^*(\vec{r}_1) \phi_{i,s}(\vec{r}_1) \phi_{j,s}(\vec{r}) |\vec{r} - \vec{r}_1| d\vec{r}_1 \\ &+ Z' \sum_{j,s} \int \frac{\phi_{j,s}^*(\vec{r}_1) \phi_{i,s}(\vec{r}_1) \phi_{j,s}(\vec{r})}{|\vec{r} - \vec{r}_1|} d\vec{r}_1 \end{aligned} \quad (26)$$

We solve for  $E$  in equation (26) iteratively and, eventually, the  $\Lambda_b$  mass is calculated from

$$M_{\Lambda_b} = m_b + 2m_{u/d} + E \quad (27)$$

The PDG value of  $\Lambda_b(5620)$  is obtained by setting the  $m_{u/d}$  to 0.157 GeV. In Table III, we

TABLE III: Comparison of  $m_{u/d}$  obtained from various lattices with quark mass parameters in the equations (20) and (26).

Lattice	$B$ meson: $m_{u/d} = 227$ MeV		$\Lambda_b$ baryon: $m_{u/d} = 157$ MeV	
	$am_{u/d}$	$m_{u/d}$ (MeV)	$am_{u/d}$	$m_{u/d}$ (MeV)
$16^3 \times 48$	0.155	204	0.105	138
$20^3 \times 64$	0.118	194	0.083	137
$28^3 \times 96$	0.087	191	0.064	143

compare the nonperturbatively tuned  $m_{u/d}$  on our lattices with those obtained by solving the equations (20) and (26). The bare lattice light quark masses cannot be directly compared to the parameter  $m_{u/d}$  in these equations mainly because of the use of renormalized  $b$  quark mass (in  $\overline{\text{MS}}$  scheme) in the Hartree-Fock calculation. Therefore, the  $m_{u/d}$ 's in the above calculation return a sort of “renormalized constituent” quark mass. Nonetheless it is obvious that we need two different  $m_{u/d}$  for two different systems, namely  $B$  and  $\Lambda_b$ . So by comparing the two sets, we simply wish to point out that the lattice tuned  $m_{u/d}$ 's are in same order of magnitude as Schrödinger equation based quark model but have a difference of 10 – 15%. This helps us to understand the possible physics behind two different tunings of light quark mass in determining the masses of single bottom hadron(s) and double bottom tetraquark.

### C. $bb\bar{u}\bar{d}$ spectrum

A plot of variation of  $bb\bar{u}\bar{d}$  mass with various  $am_{u/d}$ , including the  $\Lambda_b$  and  $B$  tuned values is shown in Fig. 3. Here we make a naive comparison of our data with the earlier quark model, lattice calculations and the PDG values, and it shows an interesting trend.

Firstly, PDG  $Z_b$ ,  $Z'_b$  and the lattice states, consisting of  $[bb]/[\bar{b}\bar{b}]$  heavy tetraquark systems, are clustered around two different masses. Our data at  $B$ -meson tuning point coincides with the PDG  $Z_b(10610)$  and  $Z'_b(10650)$  states aligning with the idea that they decay mostly

into  $\bar{B}B^*$  and  $\bar{B}^*B^*$  respectively, possibly indicating molecular nature of the state. However, our tetraquark state with  $\Lambda_b$  tuning overlaps mostly with other lattice results indicating the possibility of capturing a bound tetraquark state  $[bb][\bar{l}_1\bar{l}_2]$  much like the  $b[ll]$  state of  $\Lambda_b$ . The effective masses of the states, obtained from  $\mathcal{O}_D$  and  $\mathcal{O}_{M_1}$ , when compared with the  $B - B^*$  threshold, we find  $|D\rangle$  to exhibit a *shallow* bound state while  $|M_1\rangle$  is just marginally above. The majority of the lattice results [15–18] are found to be below this threshold as is obvious from the Fig. 3.

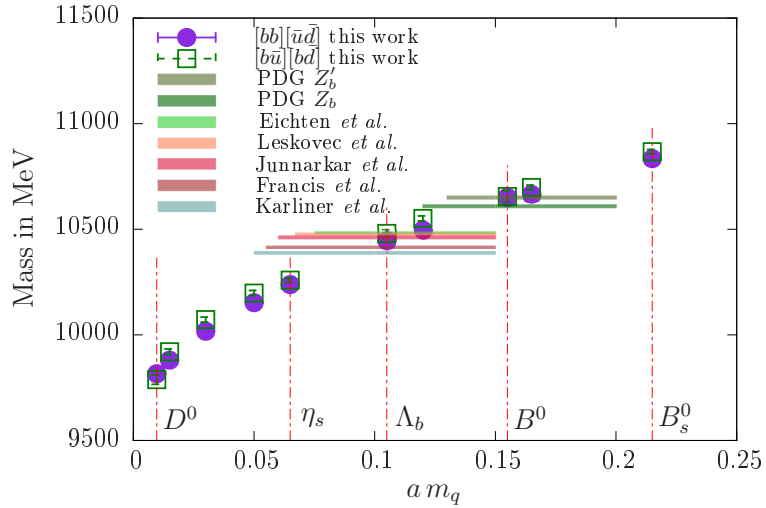


FIG. 3: Variation of  $bb\bar{u}\bar{d}$  mass at various  $am_{u/d}$  in  $16^3 \times 48$  lattice.  $\Lambda_b$ -tuned tetraquark states almost overlap with many of the quark model and lattice calculations, namely Eichten *et al.* [8], Leskovec *et al.* [18], Junnarkar *et al.* [17], Francis *et al.* [15, 16], Karliner *et al.* [44]. The  $B$ -tuned states instead coincide with  $Z_b, Z'_b$  PDG results [45].

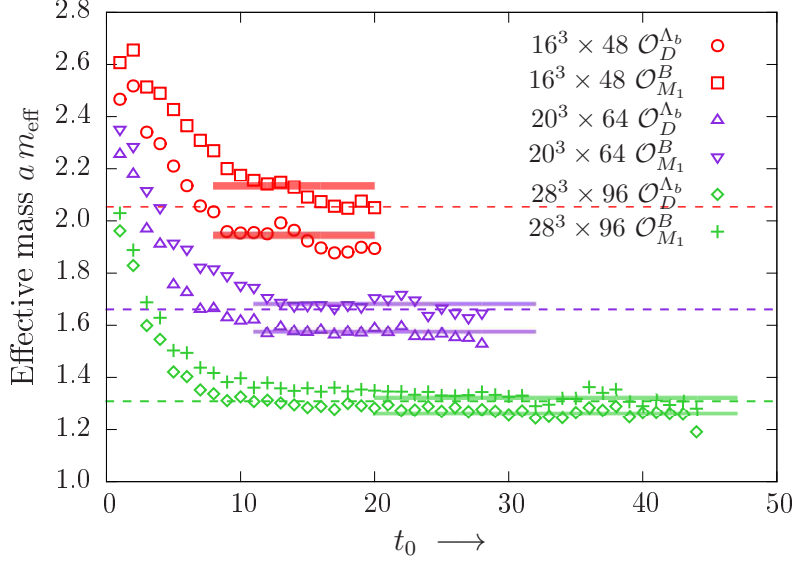


FIG. 4: Effective mass plot of the states of the operators  $\mathcal{O}_D$  and  $\mathcal{O}_{M_1}$  calculated on  $16^3 \times 48$ ,  $20^3 \times 64$  and  $28^3 \times 96$  lattices. Dashed lines are  $B - B^*$  thresholds for different lattices, see Table IV. For easy viewing, the effective masses and thresholds on  $20^3 \times 64$  (purple colored) are multiplied by a common factor of 0.85, while that of  $28^3 \times 96$  (green colored) by 0.70.

To this end, in Fig. 4 we plot the effective masses of these two states obtained at different lattice spacings. The colored bands represent fitted  $am_{\text{eff}}$  values. The superscripts  $\Lambda_b$  and  $B$  denote the light quark tuning. The dotted lines represent the lattice thresholds. The lattice threshold is defined as  $M_B + M_{B^*}$  of the non-interacting  $B - B^*$  system and consequently constructed entirely from  $B$ -meson tuned  $am_{u/d}$  and  $\Upsilon - \eta_b$  tuned  $m_b$ . We want to mention here in passing that on two occasions we used  $\Lambda_b$  tuning for operators  $\mathcal{O}_{M_1/M_2} - (i)$  to choose  $t_0$  for GEVP analysis and  $(ii)$  to determine relative contribution to the bound tetraquark ground state.

In the Table IV, we present our results of the tetraquark states corresponding to the operators given in the expressions (11, 12, 13). We call these states  $\mathcal{O}_X^\dagger |\Omega\rangle \equiv |X\rangle$  as trial states, which will later be subjected to variational analysis. The  $|\Omega\rangle$  is the vacuum state. We use two-exponential uncorrelated fit to the correlation functions, the fitting range being chosen by looking at the positions of what we consider plateau in the effective mass plots. In the columns showing various lattices, we present the masses both in lattice unit  $a E_{\text{latt}}$  and

physical unit  $M_{\text{latt}}$  in MeV, the notations being introduced in equation (6). The errors quoted are statistical, calculated assuming the lattice configurations of different lattice spacings are statistically uncorrelated. The second column shows the tuning used for the corresponding states. In the last column we provide the masses averaged over all the lattice ensembles.

TABLE IV: Masses of tetraquark states for different  $am_{u/d}$  tuning in lattice unit  $aE_{\text{latt}}$  and  $M_{\text{latt}}$  in MeV. We also include the  $B$  and  $B^*$  states that are used for threshold calculation.

Operators	Tuning	$16^3 \times 48$		$20^3 \times 64$		$28^3 \times 96$		Average (MeV)
		$aE_{\text{latt}}$	$M_{\text{latt}}$	$aE_{\text{latt}}$	$M_{\text{latt}}$	$aE_{\text{latt}}$	$M_{\text{latt}}$	
$\mathcal{O}_D = [bb][\bar{u}\bar{d}]$	$\Lambda_b$	1.944(5)	10418(7)	1.852(3)	10422(5)	1.803(5)	10407(11)	10417(9)
$\mathcal{O}_{M_1} = [b\bar{u}][b\bar{d}]$	$B$	2.133(7)	10667(10)	1.977(4)	10628(5)	1.892(6)	10602(13)	10638(27)
$\mathcal{O}_{M_2} = \epsilon_{ijk}[b\bar{u}]_j[b\bar{d}]_k$	$B$	2.124(7)	10655(8)	1.974(4)	10623(5)	1.890(5)	10560(10)	10623(35)
$\mathcal{O}_B = b\gamma_5\bar{u}$	$B$	1.022(3)	5274(4)	0.974(3)	5290(3)	0.931(3)	5268(3)	5279(10)
$\mathcal{O}_{B^*} = b\gamma_k\bar{u}$	$B^*$	1.032(3)	5288(4)	0.980(3)	5300(4)	0.938(2)	5284(3)	5292(8)
$M_B + M_{B^*}$		2.054(3)	10562(4)	1.954(3)	10590(5)	1.869(3)	10552(4)	

From the Fig. 4 and Table IV it is clear that the trial state generated by our  $\mathcal{O}_D$  operator is below  $B - B^*$  threshold which possibly indicates a bound state. On the other hand, the states for  $\mathcal{O}_{M_1}$  and  $\mathcal{O}_{M_2}$  are just above it. We tabulate the difference of the masses from their respective thresholds  $\Delta M_{D/M_1/M_2} = M_{D/M_1/M_2} - M_B - M_{B^*}$  in the Table V. In this table, we calculated the following correlator ratio to determine the mass differences which gives us an estimate of the binding energy [46],

$$C_{X-B-B^*}(t) = \frac{C_X(t)}{C_B(t) \times C_{B^*}(t)} \sim e^{-(M_X - M_B - M_{B^*})t} \quad (28)$$

It has been observed [47] that the expression (28) used to determine  $\Delta M_X$  can possibly lead to false plateaus because of  $B - B^*$  scattering states contributing differently in  $|D\rangle$ ,  $|M_1\rangle$ ,  $|M_2\rangle$  excited states which might persist at large  $t$ . In the present analysis, we have assumed these contributions are of same order of magnitude and cancel each other at moderately large  $t$ .

In the last column of Table V, we calculate our lattice average of  $\Delta M_X$  in MeV and compare with some of the previous lattice results. To our knowledge, the binding energies of the  $|M_1\rangle$

TABLE V: Mass differences of “bound”  $|D\rangle$  and “molecular”  $|M_1\rangle, |M_2\rangle$  trial states from  $B - B^*$  threshold. The subscript  $X$  denotes any of the  $D, M_1, M_2$ . The  $\Delta M_X$  are calculated from the masses and threshold given in Table IV.

Operators	Lattices	$a \Delta M_X$	$\Delta M_X$ (MeV)	$\overline{\Delta M_X}$ (MeV)
$\mathcal{O}_D$	$16^3 \times 48$	-0.125(12)	-164(16)	-167(19) this work
	$20^3 \times 64$	-0.108(10)	-177(16)	-215(12) [44]
	$28^3 \times 96$	-0.070(10)	-155(22)	-189(10) [15]
				-143(34) [17]
				-128(34) [18]
$\mathcal{O}_{M_1}$	$16^3 \times 48$	0.070(12)	92(16)	65(29) this work
	$20^3 \times 64$	0.026(11)	43(18)	see Table VI [18]
	$28^3 \times 96$	0.024(9)	53(20)	
$\mathcal{O}_{M_2}$	$16^3 \times 48$	0.070(16)	92(21)	63(30) this work
	$20^3 \times 64$	0.022(9)	36(20)	
	$28^3 \times 96$	0.020(10)	44(21)	

and  $|M_2\rangle$  states have been calculated in the framework of chiral quark model [48] for  $B - \bar{B}^*$  and  $B^* - \bar{B}^*$  states but there are no lattice results. The binding energies for the first excited states, along with the ground states, obtained on different lattice ensembles are given in [18]. Though their tuning of light quark mass is very different compared to ours, still we can use their result as a reference.

Our binding energy for the bound tetraquark state  $|D\rangle$  ( $[bb][\bar{u}\bar{d}]$ ) lies somewhere in the middle of the previously quoted lattice results. The statistical errors of the molecular states  $|M_1\rangle$  and  $|M_2\rangle$  are rather large but still they tentatively indicate non-bound molecular nature of the states. We will revisit the binding energy calculation for the molecular state(s) after variational analysis of the  $\mathcal{O}_{M_1} \times \mathcal{O}_{M_2}$  correlation matrix.

As we know, on lattice the states having the same quantum numbers can mix and, therefore, a GEVP analysis can help resolve the issue of mutual overlap of various states on the energy eigenstates. In this work, rather than the energies of the eigenstates, we are more interested to learn the overlap of our trial states, namely  $|D\rangle, |M_1\rangle$  and  $|M_2\rangle$  on the

first few energy eigenstates, where  $|0\rangle$  is the ground and  $|1\rangle, |2\rangle$  etc. are the excited states.

#### D. Variational analysis

For the 2-bottom tetraquark system with quantum number  $1^+$ , we consider the three local operators – “good” diquark  $\mathcal{O}_D$ , molecular  $\mathcal{O}_{M_1}$  and vector meson kind  $\mathcal{O}_{M_2}$  as defined above in the expressions (11 – 13) – to capture the ground state ( $|0\rangle, \mathcal{E}_0$ ) and possibly the first excited state ( $|1\rangle, \mathcal{E}_1$ ).

As is generally understood, these operators are expected to have overlap with the desired ground and excited states of the tetraquark system of our interest. The variational analysis can be performed to determine the eigenvalues and the eigenvectors from the states formed by lattice operators. This is typically achieved by constructing a correlation matrix involving the lattice operators  $\mathcal{O}_X$  and  $\mathcal{O}_Y$ ,

$$C_{XY}(t) = \langle \mathcal{O}_X(t) \mathcal{O}_Y^\dagger(0) \rangle = \sum_{n=0}^{\infty} \langle \Omega | \mathcal{O}_X | n \rangle \langle n | \mathcal{O}_Y^\dagger | \Omega \rangle e^{-E_n t} \quad (29)$$

where  $X, Y$  can be any two combinations of  $D, M_1, M_2$  in the expressions (11 – 13). The terms  $\langle n | \mathcal{O}_X^\dagger | \Omega \rangle$  are the coefficients of expansion of the trial states  $\mathcal{O}_X^\dagger | \Omega \rangle$ , written in terms of the energy eigenstates  $|n\rangle$  as,

$$\mathcal{O}_X^\dagger | \Omega \rangle = \sum_n |n\rangle \langle n | \mathcal{O}_X^\dagger | \Omega \rangle \equiv \sum_n Z_X^n |n\rangle \quad (30)$$

Presently, we are interested in expressing the energy eigenstates in terms of the trial states to understand the contribution of each to the former. If we confine ourselves to the first few energy eigenstates, we can write

$$|m\rangle = \sum_X v_m^X \mathcal{O}_X^\dagger | \Omega \rangle \Rightarrow \langle l | m \rangle = \delta_{lm} \approx \sum_X v_m^X Z_X^l \quad (31)$$

The  $v_m^X$  are equivalent to the eigenvector components obtained by solving GEVP w.r.t a suitably chosen reference time  $t_0$  [12],

$$C(t) v_m(t, t_0) = \lambda_m(t) C(t_0) v_m(t, t_0). \quad (32)$$

The eigenvalues  $\lambda_m(t)$  are directly related to the energy of the  $m$ -th state, *i.e.* ground and the first few excited states, of our system through the relation

$$\lambda_m(t) = A_m e^{-\mathcal{E}_m(t-t_0)} \quad (33)$$

The component of eigenvectors  $v_m(t, t_0)$  gives information about the relative overlap of the three local operators to the  $m$ -th eigenstate. The eigenvectors  $v_m$ 's are normalized to 1.

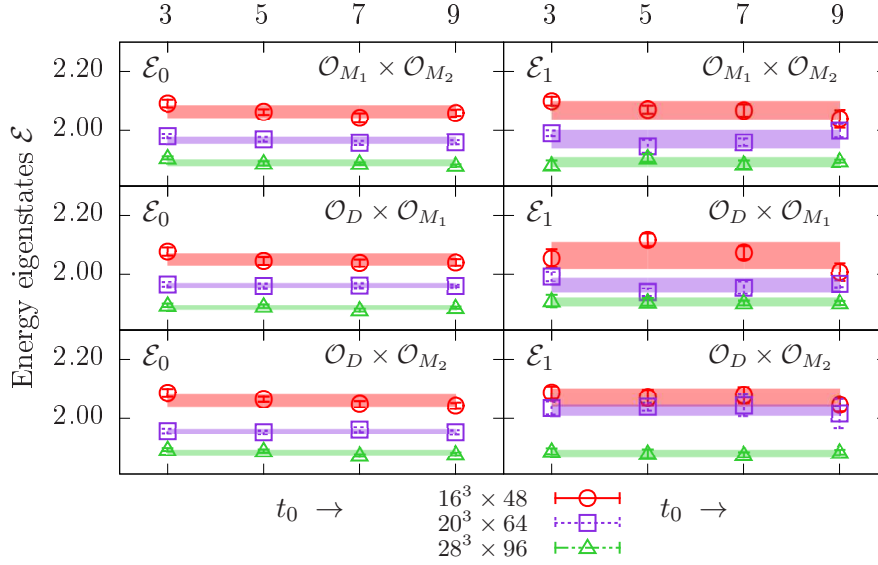


FIG. 5: Variation of ground and excited state energies  $\mathcal{E}_m$  of the equation (33) with  $t_0$ , obtained by solving  $2 \times 2$  GEVP of the correlation matrices  $\mathcal{O}_{M_1} \times \mathcal{O}_{M_2}$ ,  $\mathcal{O}_D \times \mathcal{O}_{M_1}$  and  $\mathcal{O}_D \times \mathcal{O}_{M_2}$ . In this plot we used  $\Lambda_b$ -tuned  $am_{u/d}$  for all the operators.

To determine the parameter  $t_0$ , we solve the GEVP and found that the ground and excited state energies are almost independent for  $t_0 = 3, 5, 7, 9$  as demonstrated in the Fig. 5. In this plot, we showed our results for  $\Lambda_b$ -tuned  $am_{u/d}$  for all the operators  $\mathcal{O}_X$ . As discussed before, we have used the  $\Lambda_b$  tuning whenever all three  $\mathcal{O}_D$ ,  $\mathcal{O}_{M_1}$ ,  $\mathcal{O}_{M_2}$  operators are made use of. We chose  $t_0 = 5$  for our calculations. To cross-check our choice of  $t_0$ , we also have  $B$  tuned runs and found it to be consistent.

The GEVP analysis has been carried out in two steps because of differences in the tuning of  $am_{u/d}$  for the “molecular” states  $|M_1\rangle$ ,  $|M_2\rangle$  and “good” diquark state  $|D\rangle$ . In the first step, we will do a GEVP with the  $B$ -tuned molecular operators and determine the difference of its lowest energy state from the threshold, as these states are found to coincide with experimentally observed states. In the next step, we have done the GEVP analysis with all three operators using  $\Lambda_b$  tuning to understand the state(s) below the threshold.

TABLE VI: Energy eigenvalues in lattice unit from GEVP analysis of the  $B$ -tuned  $\mathcal{O}_{M_1} \times \mathcal{O}_{M_2}$  and  $\Lambda_b$ -tuned  $\mathcal{O}_D \times \mathcal{O}_{M_1} \times \mathcal{O}_{M_2}$ .

Correlation matrix	Tuning	Energy	$16^3 \times 48$	$20^3 \times 64$	$28^3 \times 96$
$\mathcal{O}_{M_1} \times \mathcal{O}_{M_2}$	$B$ meson	$\mathcal{E}_0$	2.063(10)	1.959(12)	1.888(7)
		$\mathcal{E}_1$	2.071(10)	1.969(20)	1.906(18)
$\mathcal{O}_D \times \mathcal{O}_{M_1} \times \mathcal{O}_{M_2}$	$\Lambda_b$ baryon	$\mathcal{E}_0$	1.898(7)	1.846(5)	1.784(12)
		$\mathcal{E}_1$	1.905(10)	1.851(7)	1.816(8)
		$\mathcal{E}_2$	1.917(18)	1.856(15)	1.820(22)

In the Table VI we have shown our GEVP results of  $B$ -tuned  $\mathcal{O}_{M_1} \times \mathcal{O}_{M_2}$  and the  $\Lambda_b$ -tuned  $\mathcal{O}_D \times \mathcal{O}_{M_1} \times \mathcal{O}_{M_2}$  correlation matrices. The energy eigenstates  $\mathcal{E}_{0,1,2}$  correspond to the  $\mathcal{E}_m$  of the expression (33). In the Table VII, we calculated the energy difference of the eigenstates  $|0\rangle, |1\rangle$  etc. from their corresponding thresholds. We often find the energies of the highest states are very noisy and consequently the separation from the thresholds  $\Delta\mathcal{E}$  have large errors, hence their entries are kept vacant. We can only reliably quote the lowest for  $2 \times 2$ , and first two lowest energies for  $3 \times 3$  correlator matrices.

TABLE VII: Energy differences from the  $B - B^*$  threshold of the GEVP values of Table VI for the  $\mathcal{O}_{M_1} \times \mathcal{O}_{M_2}$  and  $\Lambda_b$ -tuned  $\mathcal{O}_D \times \mathcal{O}_{M_1} \times \mathcal{O}_{M_2}$  correlation matrices. Threshold values are taken from Table IV.

Lattice	Unit	Threshold	$\mathcal{O}_{M_1} \times \mathcal{O}_{M_2}$		$\mathcal{O}_D \times \mathcal{O}_{M_1} \times \mathcal{O}_{M_2}$		
			$\Delta\mathcal{E}_0$	$\Delta\mathcal{E}_1$	$\Delta\mathcal{E}_0$	$\Delta\mathcal{E}_1$	$\Delta\mathcal{E}_2$
$16^3 \times 48$	lattice	2.054(3)	0.010(7)	0.016(6)	-0.154(10)	-0.149(15)	-0.137(23)
(0.15 fm)	MeV	10562	13(9)	21(8)	-202(13)	-196(20)	-
$20^3 \times 64$	lattice	1.954(3)	0.010(9)	-	-0.110(9)	-0.104(10)	-0.099(19)
(0.12 fm)	MeV	10590	16(15)	-	-181(15)	-173(17)	-
$28^3 \times 96$	lattice	1.869(3)	0.012(10)	-	-0.085(10)	-0.053(10)	-
(0.09 fm)	MeV	10552	26(22)	-	-186(22)	-117(22)	-

Next we look at the contribution of  $\mathcal{O}_{M_1}$  and  $\mathcal{O}_{M_2}$  in constructing the lowest molecular

energy eigenstate  $|0\rangle$ . In the Fig. 6, we plot the histogram of the components of normalized eigenvectors  $v_0 = (v_0^{M_1}, v_0^{M_2})$  corresponding to the lowest energy  $\mathcal{E}_0$  for all three lattices. Assuming that the coefficients  $v_0^{M_1, M_2}$  approximately remain the same on all time slices and for all the individual gauge configurations of an ensemble, the histogram figures are obtained by plotting the  $M_1, M_2$  components of normalized eigenvector  $v_0$  for all time points and individual gauge configurations. As is expected, all three lattices return identical histogram of the coefficients and hence, in the subsequent histogram plots we will show only the results from  $28^3 \times 96$ . The eigenvector component  $v_0^{M_1}$  shows a peak around 0.9 indicating the lowest energy state  $|0\rangle$  receives dominant contribution from  $|M_1\rangle$  trial state. We recall here that  $\mathcal{O}_{M_1}$  corresponds to the  $B - B^*$  molecular state as defined in the equation (11).

However, the first excitation  $|1\rangle$ , for which our data is rather noisy to reliably estimate  $\Delta\mathcal{E}$ , the  $|M_1\rangle$  and  $|M_2\rangle$  states appear to have comparable contribution and are broadly distributed over different time slices and vary significantly over configurations. This is evident from the histogram plot in the Fig. 7. This may have a bearing with the fact that above the threshold, the  $Z_b$  tetraquark can couple to multiple decay channels resulting in a broad spectrum.

Including  $\mathcal{O}_D$  along with the  $\mathcal{O}_{M_1}$  and  $\mathcal{O}_{M_2}$  to form a  $3 \times 3$  correlation matrix requires using  $\Lambda_b$  tuned  $am_{u/d}$  in all three trial states. When we are exploring pure molecular states, we have used just  $\mathcal{O}_{M_1} \times \mathcal{O}_{M_2}$  correlation matrix with  $B$  tuning. But for the bound state(s) the  $\mathcal{O}_{M_1}$  and  $\mathcal{O}_{M_2}$  operators are likely to have contributions to the bound ground state along with the  $\mathcal{O}_D$ . Certainly, a  $B$ -tuned bound  $|D\rangle$  state above threshold is not well-defined and we find it has statistically small and varying overlap with the energy eigenstates much like in Fig. 7. On the other hand,  $\Lambda_b$  tuned molecular states can possibly have finite overlap to the states below the threshold. However, we always expect dominance of  $|D\rangle$  in  $|0\rangle$  because of the difference in construction of wave functions of the  $|M_1\rangle$  and  $|M_2\rangle$ .

The histogram of the eigenvector components of  $3 \times 3$  correlation matrix are shown in the Fig. 8 for the  $28^3 \times 96$  lattices. The lowest energy eigenstate  $|0\rangle$  is clearly dominated by

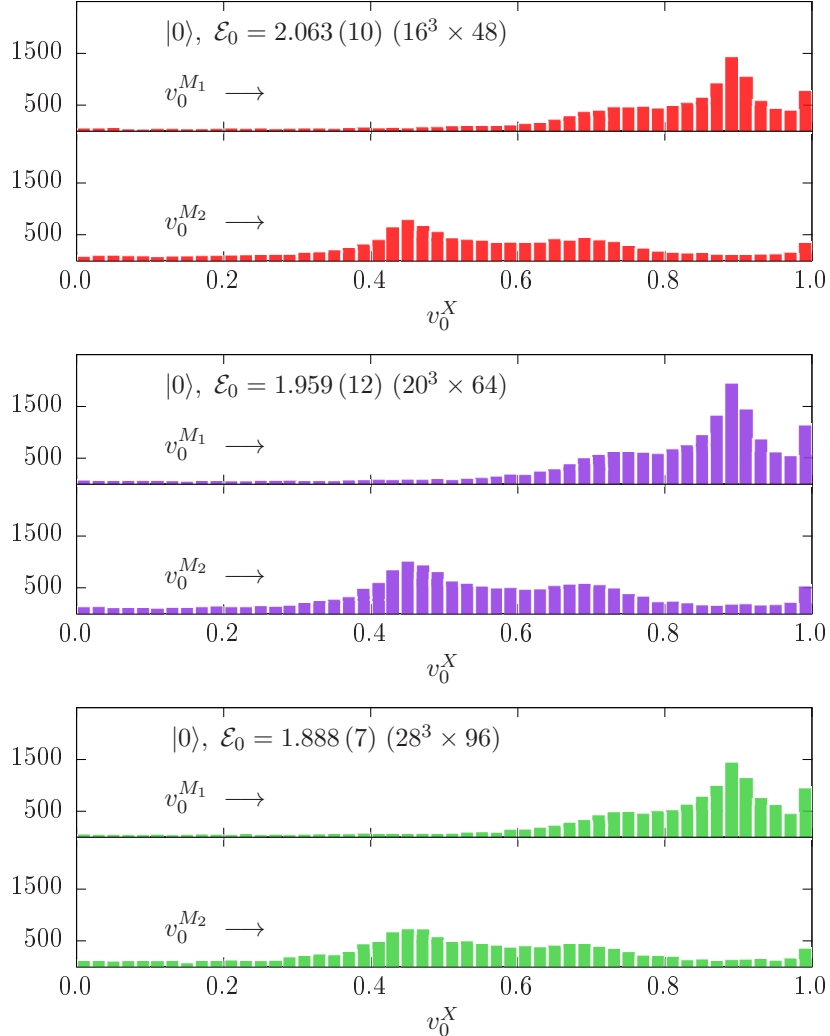


FIG. 6: The histogram plots of the normalized components  $(v_0^{M_1}, v_0^{M_2})$  which define the energy eigenstate  $|0\rangle = v_0^{M_1}|M_1\rangle + v_0^{M_2}|M_2\rangle$ .

$|D\rangle$  showing peak around 0.8, although it receives sizeable overlap from both  $|M_1\rangle$  and  $|M_2\rangle$  peaking around 0.45. But overlap of  $|D\rangle$  on  $|1\rangle$  is rather small and it is mostly molecular  $|M_1\rangle$  despite the excited state energy  $\mathcal{E}_1$  is below the threshold. Our data for  $|2\rangle$  is too noisy to extract much information. Based on this  $\Lambda_b$  tuned  $3 \times 3$  GEVP analysis, the binding energy for the ground state obtained is  $-189(18)$  MeV.

## V. SUMMARY

In this work we have attempted to study two possible  $bb\bar{u}\bar{d}$  tetraquark states – one which is bound and where most other lattice results are centered and, the other close to where

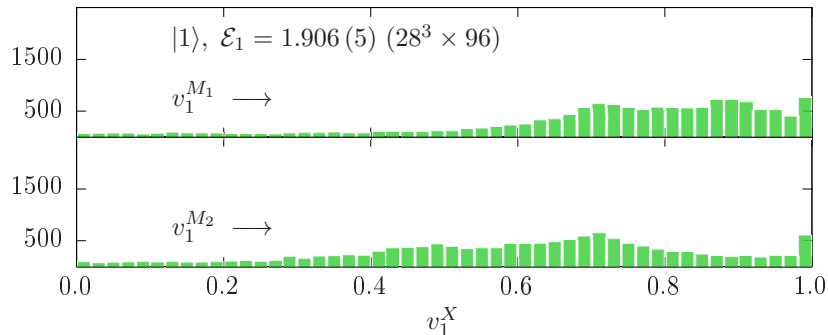


FIG. 7: The histogram plot of  $v_1^{M_1}$  and  $v_1^{M_2}$  that define the energy eigenstate  $|1\rangle = v_1^{M_1}|M_1\rangle + v_1^{M_2}|M_2\rangle$ .

PDG reports of  $Z_b$  and  $Z'_b$  are. The experimentally observed states are believed to contain a  $b\bar{b}$  pair but ours is  $bb$  pair which is considered as theoretically simpler. However, the possible molecular nature of  $Z_b$  and  $Z'_b$  suggests that our molecular states can have similar masses. For the bottom quarks we have used NRQCD action while HISQ action for the  $u/d$  quarks. This NRQCD-HISQ combination has been employed earlier in [28] for bottom meson and recently in [32] for bottom baryons. We have constructed the three lattice  $1^+$  trial states: a bound  $|D\rangle$  containing “good diquark”  $3_c$  configuration and two meson-meson molecular  $|M_1\rangle, |M_2\rangle$  with the expectation that they will contribute to the states above  $B - B^*$  threshold. There are not many lattice results on the states above threshold possibly because of the complication that they can couple to multiple decay channels besides  $B^*\bar{B}$  and  $B^*\bar{B}^*$ . Our motivation here is to obtain a tentative estimate of the  $|M_1\rangle, |M_2\rangle$  states above threshold and their relative overlap with the bound state below the threshold.

An important component of the present investigation is the tuning of the light  $u/d$  quark mass. Depending on the wave function of the operators we need two different tuning of the  $u/d$  mass. For the operators made of heavy-light  $[b\bar{l}]$  mesonic wave functions we find it is necessary to tune  $am_l$  to match  $b\bar{l}$  meson observed mass. Similarly, for light-light diquark  $[l_1l_2]$ , where  $l_1$  and  $l_2$  may or may not be equal, in presence of one or more heavy  $b$  quarks the  $am_{l_i}$  is tuned with  $\Lambda_b$ . We applied this approach with fair success in bottom baryon [32] and presently with double bottom tetraquark we attempted the same. In order to understand and explain these two different tuning, we solve the quantum mechanical Hamiltonians of  $B$ -meson system, where a single light antiquark is in the potential of a static bottom quark,

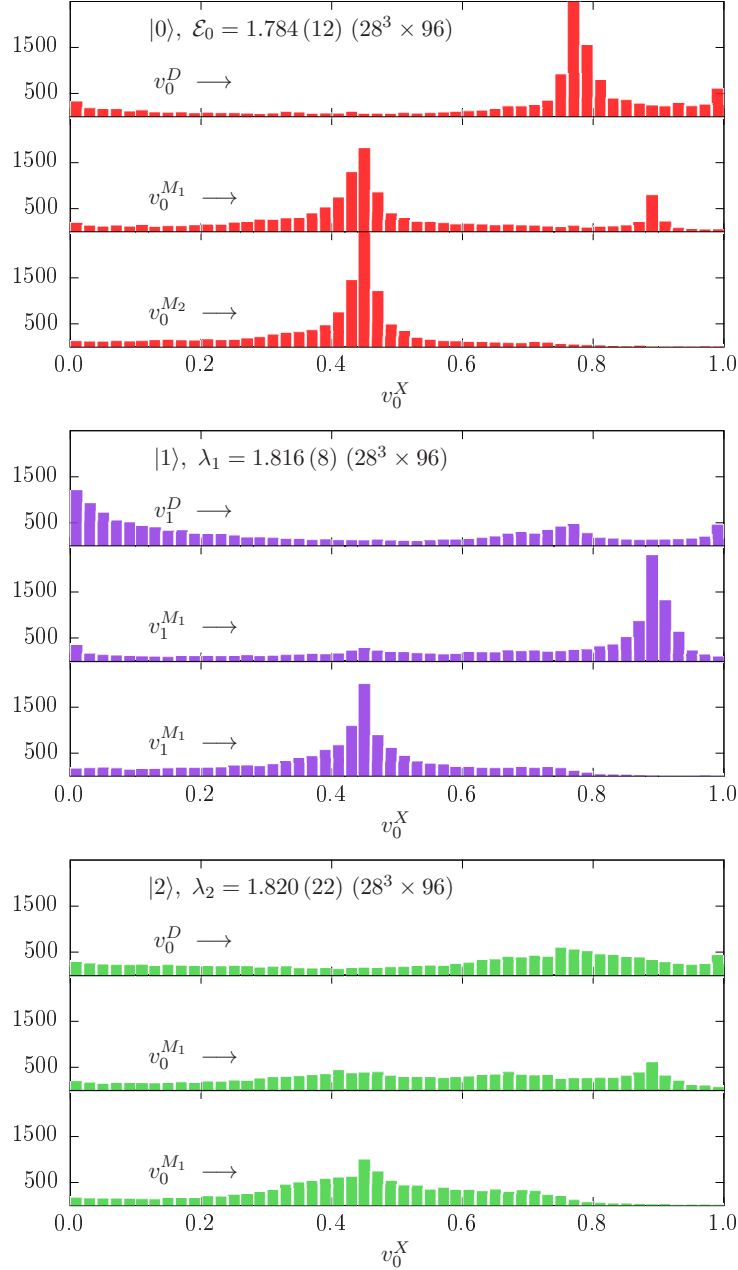


FIG. 8: Histogram plots of the normalized eigenvector components  $v_0^X$ ,  $v_1^X$  and  $v_2^X$  of  $3 \times 3$  correlation matrix, where  $X = D, M_1, M_2$ , on  $28^3 \times 96$  lattice.

and the  $\Lambda_b$ -baryon system, where the two light quarks are in the same field of the static  $b$  quark. In this problem  $b$  mass is the experimental mass and the light quark mass is treated as a parameter which is tuned to reproduce the experimental  $B$  and  $\Lambda_b$  masses. We find that the meson and baryon systems are solved for two different light quark masses which justifies our need for two different tunings. However, the actual numbers from these two sets of light

quark masses, one from solving the Schrödinger equation and the other lattice tuned, cannot be compared directly due to two different  $b$  masses used in these two instances.

Once tuned, we find the spectra of the lattice states  $|D\rangle$ ,  $|M_1\rangle$  and  $|M_2\rangle$ . Naive calculation of  $\langle \mathcal{O}_D \mathcal{O}_D^\dagger \rangle$  spectrum yields a bound state  $-167(19)$  MeV measured from the  $B - B^*$  threshold. On lattice, states having the same quantum numbers can mix and, therefore, it is natural to construct correlation matrices to solve the generalized eigenvalue problem in order to obtain the first few lowest lying energies. Besides, the components of the eigenvectors provide the relative contribution of the trial states, corresponding to the lattice operators, to the energy eigenstates. They are the coefficient of expansion of the eigenstates when expressed in terms of trial states as shown in the equation (31). The GEVP analysis reveals that tetraquark molecular state just above the threshold by only  $17(14)$  MeV is dominated by  $|M_1\rangle$  lattice state while the lowest lying bound state receives dominant contribution from  $|D\rangle$  along with significantly large contribution from both  $|M_1\rangle$  and  $|M_2\rangle$ . From  $3 \times 3$   $\Lambda_b$  tuned correlation matrix, we get our final binding energy number for  $bb\bar{u}\bar{d}$  tetraquark system to be  $-189(18)$  MeV, where the error is statistical.

## VI. ACKNOWLEDGEMENT

The numerical part of this work, involving generation of heavy quark propagators, has been performed at HPC facility in “Kalinga” cluster at NISER funded by Dept. of Atomic Energy (DAE), Govt. of India. The construction of the correlators and other analysis part of this paper has been carried out in the “Proton” cluster funded by DST-SERB project number SR/S2/HEP-0025/2010. The authors acknowledge useful discussions with Rabeet Singh (Banaras Hindu University, India) on Hartree-Fock calculation. One of the authors (PM) thanks DAE for financial support.

## REFERENCES

- 
- [1] A.E. Bondar, A. Garmash, A.I. Milstein, R. Mizuk and M.B. Voloshin, Phys. Rev. D **84**, 054010 (2011).

- [2] A. Bondar *et al.* (Belle Collaboration), Phys. Rev. Lett. **108**, 122001 (2012).
- [3] R. Aaij *et al.* (LHCb Collaboration), Phys. Rev. Lett **112**, 222002 (2014).
- [4] R.F. Lebed, R.E. Mitchell and E.S. Swanson, Prog. Part. Nucl. Phys. **93**, 143 (2017).
- [5] A. Esposito, A. Pilloni and A.D. Polosa, Phys. Rep. **668**, 1 (2017).
- [6] S.L. Olsen, T. Skwarnicki and D. Zieminska, Rev. Mod. Phys. **90**, 015003 (2018).
- [7] A.V. Manohar and M.B. Wise, Nucl. Phys. **B399**, 17 (1993).
- [8] E.J. Eichten and C. Quigg, Phys. Rev. Lett. **119**, 202002 (2017).
- [9] Y. Ikeda, B. Charron, S. Aoki, T. Doi, T. Hatsuda, T. Inoue, N. Ishii, K. Murano, H. Nemura and K. Sasaki, Phys. Lett. **B729**, 85 (2014).
- [10] Marc Wagner *et al.* 2014 J. Phys.: Conf. Ser. **503**, 012031.
- [11] M. Padmanath, C.B. Lang and S. Prelovsek, Phys. Rev. D **92**, 034501 (2015).
- [12] C. Alexandrou, J. Berlin, J. Finkenrath, T. Leontiou and M. Wagner, Phys. Rev. D **101**, 034502 (2020).
- [13] S. Prelovsek, H. Bahtiyar and J. Petkovic, Phys. Lett. B **805** (2020) 135467.
- [14] C. Hughes, E. Eichten and C.T.H. Davies, Phys. Rev. D **97**, 054505 (2018).
- [15] A. Francis, R.J. Hudspith, R. Lewis and K. Maltman, Phys. Rev. Lett. **118**, 142001 (2017)
- [16] A. Francis, R.J. Hudspith, R. Lewis and K. Maltman, Phys. Rev. D **99**, 054505 (2019).
- [17] P. Junnarkar, N. Mathur and M. Padmanath, Phys. Rev. D **99**, 034507 (2019).
- [18] L. Leskovec, S. Meinel, M. Pflaumer and M. Wagner, Phys. Rev. D **100**, 014503 (2019).
- [19] J. P. Ader, J. M. Richard, P. Taxil, Phys. Rev. D **25**, 2370 (1982).
- [20] P. Bicudo, and M. Wagner, Phys. Rev. D **87**, 114511 (2013).
- [21] P. Bicudo, K. Cichy, A. Peters, B. Wagenbach and M. Wagner, Phys. Rev. D **92**, 014507 (2015).
- [22] P. Bicudo, J. Scheunert and M. Wagner, Phys. Rev. D **95**, 034502, (2017).
- [23] P. Bicudo, M. Cardoso, A. Peters, M. Pflaumer and M. Wagner, Phys. Rev. D **96**, 054510 (2017).
- [24] B.A. Thacker and G.P. Lepage, Phys. Rev. D **43**, 196 (1991).
- [25] G.P. Lepage, L. Magnea, C. Nakhleh, U. Magnea and K. Hornbostel, Phys. Rev. D **46**, 4052 (1992).
- [26] E. Follana, Q. Mason, C. Davies, K. Hornbostel, G.P. Lepage, J. Shigemitsu, H. Trotter and K. Wong, Phys. Rev. D **75**, 054502 (2007).

- [27] A.X. El-Khadra, A.S. Kronfeld and P.B. Mackenzie, Phys. Rev. D **55**, 3933 (1997).
- [28] E.B. Gregory *et al.* (HPQCD Collaboration), Phys. Rev. D **83**, 014506 (2011).
- [29] N. Kawamoto and J. Smit, Nucl. Phys. B **192**, 100 (1981).
- [30] J. Jiang, W. Chen and S. Zhu, Phys. Rev. D **96**, 094022 (2017).
- [31] R.L. Jaffe, Phys. Rep. **409**, 1 (2005).
- [32] P. Mohanta and S. Basak, Phys. Rev. D **101**, 094503 (2020).
- [33] A. Bazavov *et al.*, Rev. Mod. Phys. **82**, 1349 (2010).
- [34] K. Orginos and D. Toussaint (MILC), Phys. Rev. D **59**, 014501 (1998).
- [35] K. Orginos, D. Toussaint, and R. L. Sugar (MILC), Phys. Rev. D **60**, 054503 (1999).
- [36] K. C. Bowler *et al.*, (UKQCD Collaboration), Phys. Rev. D **54**, 3619 (1996).
- [37] B.C. Tiburzi, Phys. Rev. D **71**, 034501 (2005).
- [38] Z.S. Brown, W. Detmold, S. Meinel, and K. Orginos, Phys. Rev. D **90**, 094507 (2014).
- [39] S. Godfrey and N. Isgur, Phys. Rev. D **32**, 189 (1985).
- [40] S. Capstick and N. Isgur, Phys. Rev. D **34**, 2809 (1986).
- [41] [folk.uib.no/nfylk/Hartree/lindex.html](http://folk.uib.no/nfylk/Hartree/lindex.html)
- [42] D. R. Hartree and W. Hartree, Proc. R. Soc. Lond. A **150**: 9–33, (1935).
- [43] V. Fock, Z. Physik **61**, 126–148 (1930).
- [44] Marek Karliner and Jonathan L. Rosner, Phys. Rev. Lett. **119**, 202001 (2017)
- [45] M. Tanabashi *et al.* (Particle Data Group), Phys. Rev. D **98**, 030001 (2018) and 2019 update.
- [46] S.R. Beane, K. Orginos, and M.J. Savage, Phys. Lett. B **654**, 20 (2007).
- [47] T. Iritani *et al.* (HAL QCD Collaboration), JHEP **1610** (2016) 101.
- [48] G. Yang, J. Ping, and J. Segovia, Phys. Rev. D **101**, 014001 (2020)